Bidirectional coupling of electromagnetic and thermal processes in radiofrequency hyperthermia

M. Morega*, M. Neagu**, Al. Morega*
* POLITEHNICA University of Bucharest/Electrical Engineering Department, Bucharest, Romania
** National Institute of Metrology, Bucharest, Romania

Abstract—**Hyperthermia and coagulation therapies are based on the tissue heating and represent minimally invasive medical procedures; they are recommended for the treatment of tumors in soft tissues (liver, kidney, breast, etc.). The energy is delivered to the tissue through a microwave (MW) thin antenna, inserted transcutaneously. Both procedures require a careful preparation for the intervention; the power and frequency of the MW source, the design of the antenna, the time interval while the energy is delivered are some significant factors that determine the temperature distribution in the target tissue. Numerical modeling of the intervention is a research tool, useful for the optimization of the procedure. The coupled phenomena, electromagnetic and thermal, are analyzed here in a numerical experiment with the finite element method (FEM); electromagnetic field (EMF), absorbed power density and temperature distributions are computed inside the exposed volume of tissue and the energetic efficiency of the applicator is evaluated.**

I. INTRODUCTION

Thermal effects, that occur when the human body (considered as a conductive dielectric medium) is exposed to EMF in the MWs frequency range (10^8 – 10^{11} Hz), could be used in medicine, to treat tumors either through hyperthermia or through coagulation procedures. Hyperthermia provides the rise of the temperature in the tumorous tissue to 43 – 45 ^{0}C for extended periods of time (minutes or even hours), while metabolic changes are expected to occur in metastatic cells, aiming at their destruction [1, 2]. Coagulation assumes a temperature rise over 60 ^{0}C for only a few minutes and leads to the annihilation of the tumor by necrosis. The use of heat to reduce or eliminate tumors has been known for more than a century, but only in the past three decades the means for accomplishing reasonably controlled heating have been available [3 - 7].

Heating as a consequence of the exposure to MWs is explained by the energy transferred to the target tissue via capacitive coupling, which causes vibration of polar particles, mainly the water molecules. Tumorous tissue is especially hydrated and becomes the region that preferentially concentrates heat. The design of the applicator should correlate the technical factors (working frequency, delivered power and antenna geometry) that could correspond to the best coupling between the applicator and the target tissue in order to provide the optimum control of the treatment. For better results, hyperthermia is currently associated to the action of ionizing radiation, ultrasounds, or to chemotherapy.

The main limitation of MWs hyperthermia is due to the difficulty in obtaining reliable and uniform heating at deep tissue sites. The operating frequency is usually 2.45 GHz, which is one of the frequencies dedicated to ISM (Industrial, Scientific, and Medical) applications. MW radiation has a low penetration depth in anatomical tissues, on the order of 0.015 – 0.025 m [8, 9]; consequently, external applicators manifest the inability to deliver uniform thermal doses to tumor volumes. As a solution to that problem, local interstitial techniques have been developed that are proving to be safe and effective. These techniques employ implanted minimally invasive thin antennas for the delivery of local thermal doses; they are inserted through the skin, into a biocompatible catheter, under the guidance provided with an imaging monitoring procedure (for example ecography) [7, 8].

In dosimetric estimation, numerical modeling and experiment are complementary investigation methods. Measurements of the electric field strength or derived quantities provide limited data, due to the inherent sensibilities and uncertainties of the experiment and to the difficulties of measuring inside the target tissue. Numerical modeling is the most suited method for the evaluation and optimization of medical technology based on tissue exposure to EMF; after the validation of the model, it is possible to try a large spectrum of exposure conditions and to evaluate dosimetric quantities at each location inside the exposed body.

The paper presents the numerical model and evaluates the distribution of the dosimetric parameters inside the exposed tissue, as much as the connection between the power delivered by the electromagnetic field source and the heating of the tissue. The exposed tissue is modeled as a lossy dielectric material, with temperature and frequency dependent properties. In that case, EMF and thermal problems are coupled in a bidirectional manner; when the time dependent heating process is evaluated, the EMF problem characterized by adjusted material properties should be solved for each temperature step. Chang explores in [6] the relevance of considering temperature dependent conductivity in radiofrequency ablation and concludes that the temperature influence is not at all negligible. However, our study takes a different approach in approximating the temperature sensitive tissue electric properties (both the electric conductivity and the dielectric permittivity) and applies the procedure to low thermal variations, specific to hyperthermia medical procedure.

II. NUMERICAL MODEL

We analyzed the case of hepatic tissue, exposed to EMF at 2.45 GHz, radiated by a needle antenna surrounded by a protective catheter and inserted trans-cutaneously in the liver [7]. The antenna is built as a coaxial cable, short-circuited at the end and having a circular radiant slot; its geometry and dimensions are presented in fig. 1. The geometry of the antenna was previously optimized with regard to the best energetic coupling (i.e. maximum energy transmitted) between the MWs source and the exposed tissue [8].

The EMF problem is solved for the magnetic field strength $\underline{\mathbf{H}}$, in time-harmonic regime of electromagnetic waves (in complex representation)

$$\nabla \times \left(\underline{\varepsilon}^{-1} \nabla \times \underline{\boldsymbol{H}} \right) - \omega^2 \mu_0 \underline{\boldsymbol{H}} = 0, \qquad (1)$$

with the angular frequency $\omega = 2\pi f$, inside the exposed tissue modeled as a nonmagnetic and conductive dielectric material, with the complex electric permittivity $\underline{\varepsilon} = \varepsilon_0 \varepsilon_r - j\sigma/\omega$ and the magnetic permeability $\mu_0 = 4\pi 10^{-7}$ H/m. We considered the temperature dependence of the electric conductivity σ and relative permittivity ε_r, suggested in [10] for anatomical tissues with high water content; the reference values (σ and ε_r at the normal body temperature, 37°C, and working frequency, 2450 MHz) could be found in [11], the most cited database of anatomical tissue properties. The hepatic tissue is represented as a cylindrical volume surrounding the antenna, and the computational domain is limited, far enough from the antenna, by low reflecting boundary conditions

$$\boldsymbol{n} \times \left(\nabla \times \underline{\boldsymbol{H}} \right) - j\omega \sqrt{\varepsilon_0 \mu_0} \left(\underline{\boldsymbol{H}} - \left(\boldsymbol{n} \cdot \underline{\boldsymbol{H}} \right) \boldsymbol{n} \right) = 0. \qquad (2)$$

The source of MWs is defined by specifying the magnetic field strength in a cross-section of the cylindrical antenna, acting as a waveguide with TM propagation mode (the vector $\underline{\mathbf{H}}$ has only an azimuthally oriented component $\underline{\mathbf{H}} = \mathbf{e}_\varphi \underline{H}_{\varphi 0}$); the expression of the magnetic field strength is the analytical solution of the propagation problem in the cylindrical waveguide

$$\underline{H}_{\varphi 0} = \frac{1}{r} \sqrt{\frac{P_{in}}{\underline{Z}} \cdot \frac{1}{\pi \log \frac{r_2}{r_1}}}, \qquad (3)$$

with r_1 and r_2 the values of the inner and outer radial coordinate r of the cylindrical antenna, $\underline{Z}$ the wave impedance in the dielectric material where it propagates and P_{in} the power delivered by the MWs source.

In a convenient arrangement, the 3D problem presents axial symmetry and could be treated in 2D.

The time dependent thermal problem follows a classical Pennes equation [12]

$$\rho C \frac{\partial T}{\partial t} = k \nabla^2 T - \rho \rho_b C_b F \left(T - T_b \right) + \rho SAR, \qquad (4)$$

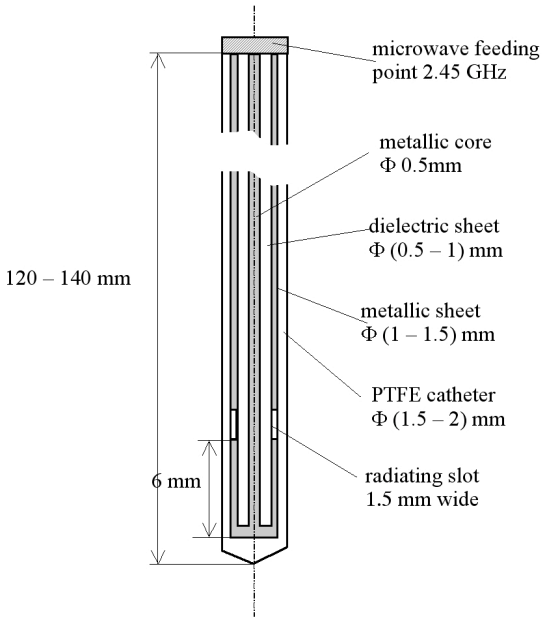

Figure 1. Design characteristics of the microwave applicator (coaxial antenna with radiating slot)

which considers that the thermal increase is due to the effects of the conductive heat transfer through the hepatic tissue, the blood perfusion and the energy intake from the MWs source. In eq. (3), T and T_b are the temperatures of the thermally treated tissue and of the blood, t is the time, ρ and ρ_b represent the mass densities of the tissue and blood, C and C_b are the specific heat coefficients of the tissue and blood, k represents the thermal conductivity of the tissue and F is the blood flow rate. The heating source is introduced through the specific energy absorption rate

$$SAR = \sigma E^2 / \rho, \qquad (5)$$

where E stands for the rms value of the electric field strength (computed as a derived quantity).

The physical properties are referred in Table 1.

TABLE I. PHYSICAL PROPERTIES USED IN THE MODEL.

Hepatic tissue		
$\sigma(T) = 1.66 \cdot \left[1 + 0.005 \cdot (T - 310) \right] \ \frac{\mathrm{S}}{\mathrm{m}}$		
$\varepsilon_r(T) = 42.6 \cdot \left[1 - 0.027 \cdot (T - 310) \right]$		
$\rho = 1060 \ \frac{\mathrm{kg}}{\mathrm{m}^3}$	$C = 3600 \ \frac{\mathrm{J}}{\mathrm{kg} \cdot {}^{\mathrm{o}}\mathrm{C}}$	$k = 0.502 \ \frac{\mathrm{W}}{\mathrm{m} \cdot {}^{\mathrm{o}}\mathrm{C}}$
Blood		
$\rho_b = 1000 \ \frac{\mathrm{kg}}{\mathrm{m}^3}$	$C_b = 4180 \ \frac{\mathrm{J}}{\mathrm{kg} \cdot {}^{\mathrm{o}}\mathrm{C}}$	$F = 6.4 \cdot 10^{-6} \ \frac{\mathrm{m}^3}{\mathrm{kg} \cdot \mathrm{s}}$
PTFE catheter and cable dielectric		
$\sigma_{PTFE} = 0, \ \sigma_{dielec} = 0$	$\varepsilon_{r\ PTFE} = 2.6, \ \varepsilon_{r\ dielec} = 2.03$	

Due to the temperature dependent electric properties of the hepatic tissue, eqs. (1) and (4) are interrelated. The numerical solution of the model is obtained in COMSOL Multiphysics, based on the FEM [13].

In the absence of original experiments, our 3D FEM model was validated trying to replicate computational and experimental results presented in literature. On the basis of the model design specified above, we created a 3D FEM model for the EMF problem presented in [7]; we took advantage of the detailed information offered there and considered the generic model introduced in the cited paper, as a benchmark type application.

The solution of our FEM numerical EMF computation exhibits a remarkable concordance with the experimental and numerical results shown in [7]; fig. 2 proves the satisfactory output of this analysis. *SAR* is determined in the volume surrounding the applicator and its distribution is plotted along the "observation line" defined in the picture (a). The graphs (b) display the *SAR* plots ("normalized" means true *SAR* values rated to the maximal value located on the observation line). Paper [7] exhibits three concordant types of results: numerical with FEM and FDTD methods and experimental; our solution (c) fits to the same distribution form, and it complies most with the FEM solution reported in [7].

III. DOSIMETRIC ESTIMATES

The distribution of *SAR* for the antenna inserted in the hepatic tissue was computed with the 3D FEM model described earlier (physical properties at 37^0C and 1W delivered power). We checked further the validity of the axial symmetry, comparing the slice-plots of *SAR* computed with the 3D versus the 2D model (based on axial symmetry) and the spectra are displayed in fig. 3. As one could see, the 2D FEM model has a proper accuracy and it is much more economic than the 3D one; consequently, it will be used for further analysis of homogeneous tissue, while the 3D model will find its usefulness in nonhomogeneous problems, when tumor-like subdomains will be included inside the target volume of tissue.

SAR computation with our 2D model was also employed for an estimation of the EMF and thermal coupled problem solution stability at small oscillations of the electrical conductivity, in the limit of ±10% around the given value (i.e. $\sigma = 1.66$ S/m and $\varepsilon_r = 42.6$, at 2.45 GHz and 37^0C, as specified in Table 1). Tissue electrical properties are currently determined through experiment, on excised anatomical samples and measured results are highly dependent on the experimental conditions and the quality of the sample, as the literature illustrates.

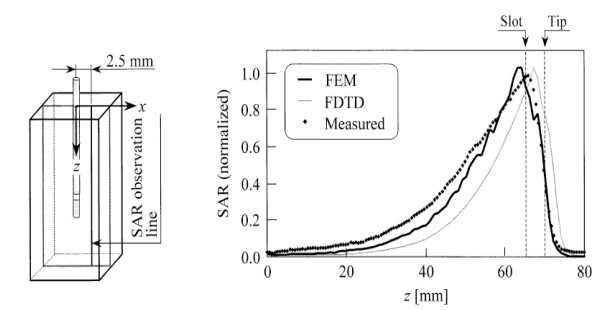

(a) SAR observation line. (b) Calculated and measured SAR distributions.

Copy of fig. 5 from paper [7]

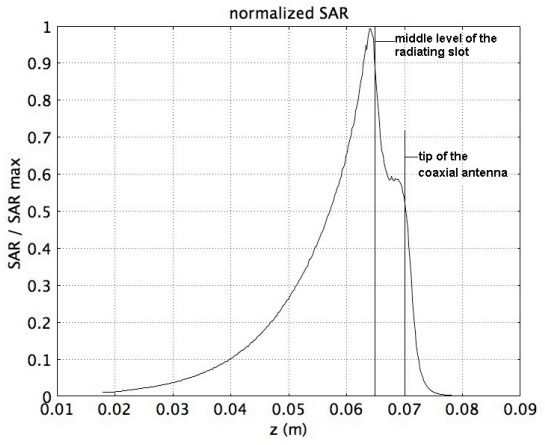

(c) *SAR* distribution on the observation line with our model

Figure 2. Validation of the 3D FEM model used here, against the model analysed in literature [7]

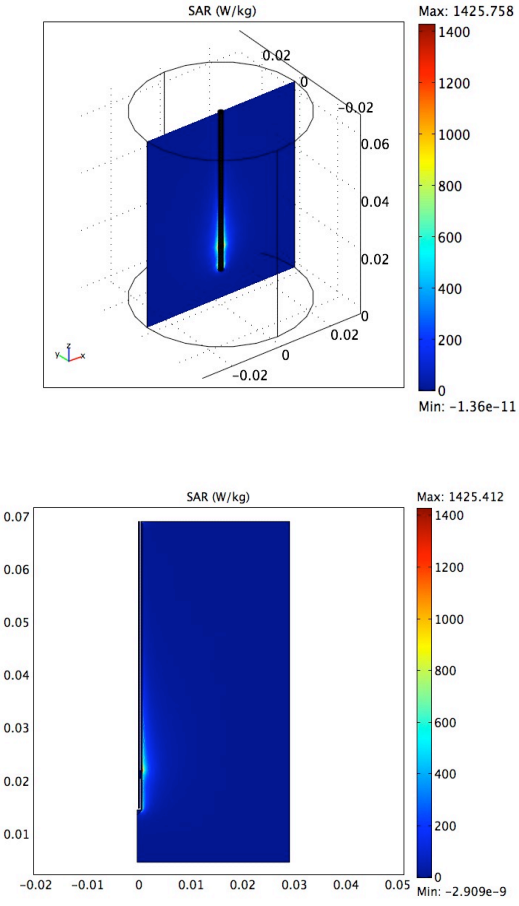

Figure 3. SAR distribution in the plane of axial symmetry of the model (3D model – up and 2D model – down)

Consequently, the differences among the values found in public databases is significant. Another reason for considering properties dispersion is the variation of the electric properties (especially conductivity) with the water content of tissue (tumorous tissue is more hydrated than healthy tissue, and anatomical tissues usually loose water with the ageing). Fig. 4(a) shows the *SAR* plots along an "observation line", which is traced parallel to the antenna, at 0.5 mm distance, from the antenna tip (z = 0.014 m) up to the level of its incidence into the domain (z = 0.065 m); the four curves correspond to different electric conductivities of the hepatic tissue. The spikes appear slightly above the level of the radiating slot, due to interference effects; the larger differences in *SAR* values occur at the same level. As one could observe, approx. 5% variation of the conductivity leads to almost the same variation in *SAR*; this is explained by the direct dependency between *SAR* and the conductivity, eq. (5), while the electric field solution is practically unaffected by the same variations of the conductivity, as fig. 4(b) shows (the four *E* plots are almost superposed). The temperature variation is also important, and fig. 4(c) displays the corresponding temperature distributions along the observation line. The temperature gradient is different from the *SAR* gradient on the observation line and the most affected hepatic tissue region is the one in the immediate proximity of the antenna slot.

We performed further the same tests relative to small variations of the permittivity. Unlike the variation of conductivity, the permittivity dispersion does affect the electric field solution; a decrease in the value of the permittivity leads to the rise of the electric field strength and consequently, determines the rise of *SAR* and temperature, as fig. 5 shows in similar representations as those in fig. 4. Both sets of characteristics need to be analyzed in parallel, in order to conclude on the dispersion of the dosimetric quantities at small variations of the biological materials electric properties.

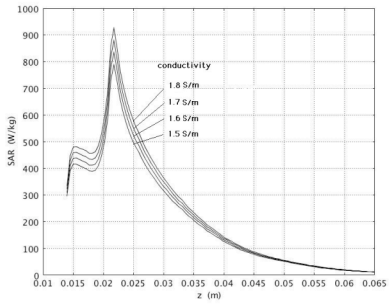

(a) *SAR* distributions

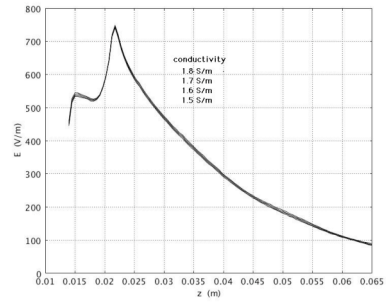

(b) *E* distributions (r.m.s. values of time harmonic *E*-field)

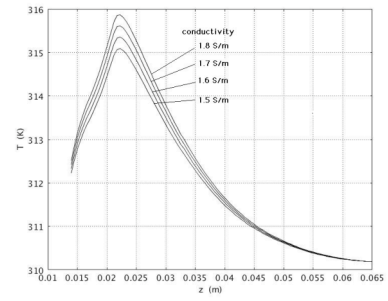

(c) *T* distributions

Figure 4. *SAR, E* and *T* distributions along the antenna, at a distance of 0.5 mm, for different electric conductivities of the hepatic tissue (2.45 GHz, 1W)

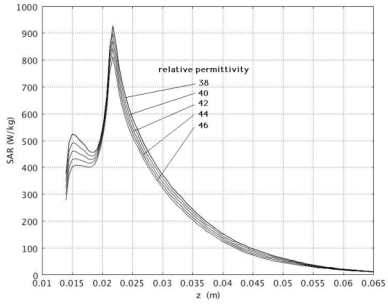

(a) *SAR* distributions

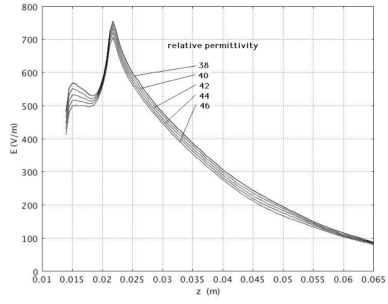

(b) *E* distributions (r.m.s. values of time harmonic *E*-field)

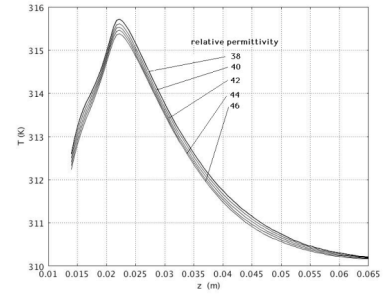

(c) *T* distributions

Figure 5. *SAR, E* and *T* distributions along the antenna, at a distance of 0.5 mm, for different relative permittivities of the hepatic tissue (2.45 GHz, 1W)

IV. COUPLED EMF AND THERMAL PROBLEMS

When coupling the EMF and the thermal field problems we compared the two cases:

(1) *unidirectional coupling*, with constant physical properties – temperature does not affect electrical properties and the EMF problem is solved once (*SAR* remains constant, while the thermal field problem follows the transient process)

(2) *bidirectional coupling*, where the electric conductivity and permittivity depend on the temperature, as Table 1 shows and the EMF and thermal problems are solved and interconnected for each time step (respectively for each temperature, with adequate electrical properties).

We estimated the temperature rise dependency on the power of the MWs source, in both coupling cases; the results are illustrated in fig. 6. The hot spot highest temperature allowed in hyperthermia, 45^0C (318 K), is reached for the power of 1.43 W in the case of constant electric properties (unidirectional coupling) and for the power of 1.2 W for temperature dependent properties (bidirectional coupling).

The time dependent heating reaches a stationary state after approx. 500 s, when the MWs source delivers the constant power of 0.9 W; we have analyzed these conditions too, and observed that the stabilized temperature is 42.5^0C (315.5 K) for the unidirectional coupling case and 43.1^0C (316.1 K) for the bidirectional one, as fig. 7 shows in the slice-plots of the temperature distribution. Even though the differences are in the inherent error margins introduced by the dispersion of data, we consider that the computational effort is worthy to enhancing the precision of the analysis, with the hope that future research in this domain will provide more specific data for the anatomical tissue properties.

We consider *the target volume in hyperthermia* defined as the tissue volume heated between 43 and 45 ^{o}C, that means (316 - 318) K. This target volume was numerically identified around the antenna, on the solution of the unidirectional coupling problem, when the MWs source power is 1.43 W (see fig. 6); its dimension is approx. 200mm^3, while for the bidirectional coupling problem, at the power of 1.2 W, its dimension is 110 mm^3.

Another test performed for the heating estimate in tissues with temperature dependent properties refers to the case of a nonhomogeneous hepatic tissue, due to the

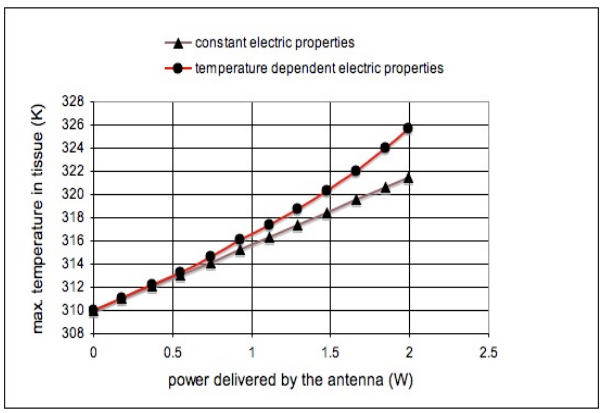

Figure 6. Hot spot temperature in the model of the exposed hepatic tissue, for the two coupling cases

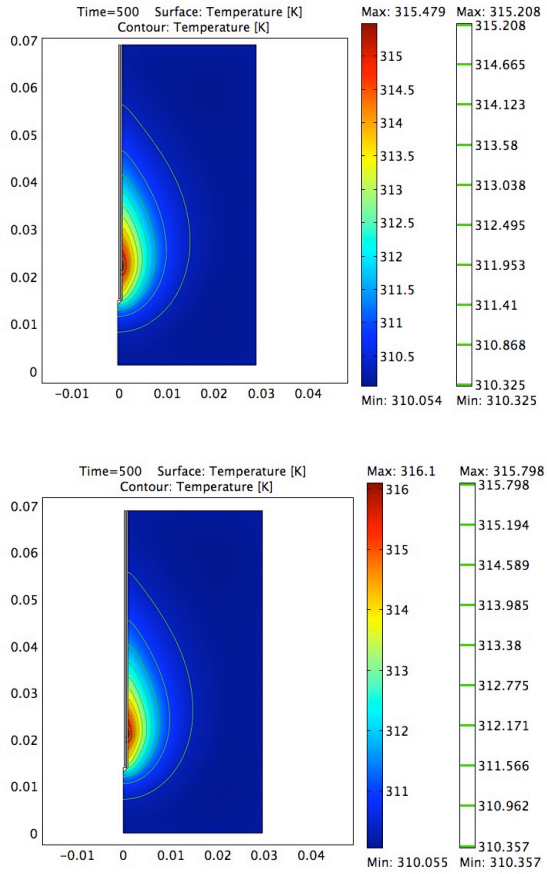

Figure 7. Temperature distributions at 0.9 W, for constant electrical properties (up) and temperature dependent electrical properties (down)

occurrence of tumoral inclusions. Since a tumor is more hydrated than healthy tissue, its electric conductivity is approx. 30% higher comparative to healthy tissue, according to impedance measurements.

Our study considers the presence of some inclusions represented as small spheres, spread around the MWs applicator; their number and characteristic dimension is randomly generated here, as well as the distance from the applicator. We considered three spheres with different diameters (1, 2 and 3 mm) comparable to the diameter of the MWs antenna; all the three spheres are centered at the same level on the *z*-axis, namely at the level of maximal exposure (see *E*, *SAR* and *T* spikes in fig. 4 and 5). Due to the lack of any symmetry in the new configuration, the 3D FEM model should be employed this time (see fig. 8 for the geometrical configuration). The electric conductivity introduced earlier, $\sigma = 1.66$ S/m, at 2.45 GHz and 37^0C, (as specified in Table 1) is assigned to the tumorous inclusions, while the electric conductivity for the rest of the hepatic tissue is lower, $\sigma^* = 1.2$ S/m, as [11] indicates for normal tissue at the same temperature and frequency.

We computed the absorbed power and the average temperature inside the three spherical inclusions with the 3D FEM model and the bidirectional coupling of the EMF and thermal problems. When the total MWs power delivered to the system is $P_{in} = 1$W, we found that the

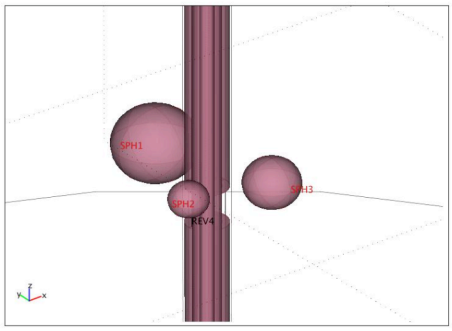

Figure 8. Detail of the 3D FEM model geometry (cylindrical antenna with radiating slot and three spherical inclusions)

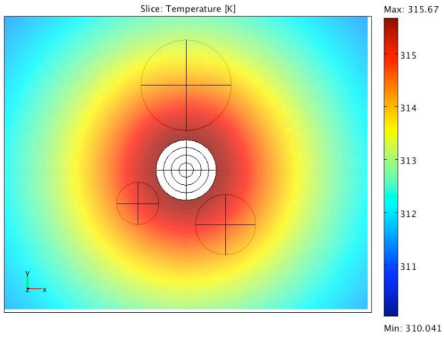

Figure 9. Temperature distribution in the cross-sectional plane located at the level with higher exposure intensity

power absorbed in the spheres with higher conductivity represents 6.6% of it, compared with 5.1% for the case of spherical inclusions with the same conductivity as the rest of the liver; the average temperature of the spheres is 314 K in the first case, and 313.7 K in the second one. Fig. 9 shows the temperature distribution in a cross-sectional plane, in the region of maximal exposure to MWs, at the end of the heating process (the temperature is stabilized). As expected, the higher conductive tissue does not concentrate the electric field, and the accumulated power and temperature rise are nonsignificant.

V. CONCLUSIONS

As illustrated by the analysis performed here, the numerical modeling of hyperthermic treatment of tumors is highly dependent on the accuracy of the model design, especially when it comes to define the anatomical media properties. A numerical model could facilitate the therapeutic forecast and optimization, being also able to provide data that are impossible to be measured, or to complement experimental data. The control of parameters (material properties) represents the fundamental condition for the applicability of the model. As the documentation performed by the authors reveals, the scientific research in that domain is still in progress.

A numerical model based on the FEM computation is presented in the paper, together with some preliminary results directed to validation of that model and to the estimation of the solution sensibility in relation to the dispersion of material properties.

The research is further focused on the analysis of the relation between the applied power from the MWs generator and the temperature level obtained in hyperthermia treatment of tumorous hepatic tissue. Two types of problem formulations were compared: the coupling between the EMF and the thermal field, when *not considering* the temperature dependency of the electrical properties (conductivity and permittivity) of hepatic tissue, against *considering* this dependency. The differences between the results in the two coupling cases seem to be small, but the control of the temperature is crucial in hyperthermia. Since the value of 318 K (45 ^{o}C) is the maximum allowed by the treatment protocol, the risk to increase the temperature above this limit could produce damage of the healthy tissue and could be harmful for the patient.

ACKNOWLEDGMENT

This work was performed in the Laboratory for Electrical Engineering in Medicine, POLITEHNICA University of Bucharest, and it was supported through the CNCSIS research grant A - 357/2007.

REFERENCES

[1] K. R. Foster, A. Lozano-Nieto, P. J. Riu, "Heating of tissues by microwaves: a model analysis," *Bioelectromagnetics*, vol.19, pp. 420-428, 1998

[2] Urano M., Douple E. (Editors), *Hyperthermia and Oncology, Thermal Effects on Cells and Tissues*, Brill Academic Pub. 1988, ISBN 9067640875

[3] Bini M., Feroldi P., Olmi R., Pasquini A., "Electromagnetic diathermy: a critical review," Phys Med 1994, X: 39-46.

[4] Hildebrandt B., Wust P., Ahlers O. et al., "The cellular and molecular basis of hyperthermia," Critical Reviews in Oncology/Hematology, vol 43, pp.33–56, 2002

[5] Kenneth R. Foster, Albert Lozano-Nieto, Pere J. Riu, "Heating of Tissues by Microwaves: A Model Analysis," Bioelectromagnetics, vol. 19, pp.420-428, 1998

[6] I. Chang. "Finite element analysis of hepatic radiofrequency ablation probes using temperature-dependent electrical conductivity," *BioMedical Engineering OnLine* , 2:12, 2003

[7] K. Ito, K. Saito, T. Taniguchi, H. Yoshimura, "Temperature distribution in and around array applicator for interstitial microwave hyperthermia combined with interstitial radiation therapy," Proc. of the 27th Intl. URSI Gen. Assembly, Maastricht, 2002

[8] M. Morega, L. Mogos, M. Neagu, A. Morega, " Optimal Design for Microwave Hyperthermia Applicator," Proc. of the 11th Intl. Conf. on Optimization of Electrical and Electronic Equipment - OPTIM 2006, ISSN 0093-9994, Brasov, Romania, May 2006, vol. I Electrotechnics, ISBN 973-635-703-1, 978-973-635-703-9, p. 219-224

[9] M. Morega, A. Morega, A. Machedon, "Simplified numerical models for microwave dosimetry in human tissue," 3rd European Medical and Biological Engineering Conf. EMBEC'05&IFMBE, Praga, Czech Rep., IFMBE Proceedings CD-ROM, ISSN 1727-1983, nov. 2005

[10] Nikawa Y., "Temperature Depending SAR Distribution in Human Body During Hiperthermia Treatment", IEICE Trans. Electron. vol. E78-C, no. 8, August 1995

[11] C. Gabriel, S. Gabriel, "Dielectric properties of body tissues at RF and microwave frequencies," Report for Armstrong Laboratory (AFMC), Occupational and Environmental Health Directorate - Radiofrequency Radiation Division, USA, 2002G. (www.brooks.af.mil/AFRL/HED/hedr/reports/dielectric)

[12] H. H. Pennes, "Analysis of tissue and arterial blood temperature in the resting human forearm," *J. Appl. Phys*., vol.1, pp.93-122, 1948

[13] COMSOL Multiphysics® v. 3.3a, Users' Guide, RF Module, Heat Transfer Module, 2007